

**Condensational and collisional growth of cloud droplets in a turbulent environment<sup>†</sup>**

XIANG-YU LI\*

*Department of Meteorology and Bolin Centre for Climate Research, Stockholm University, Stockholm, Sweden;  
 Nordita, KTH Royal Institute of Technology and Stockholm University, 10691 Stockholm, Sweden;  
 Swedish e-Science Research Centre, www.e-science.se, Stockholm, Sweden;  
 JILA and Laboratory for Atmospheric and Space Physics, University of Colorado, Boulder, CO 80303, USA*

AXEL BRANDENBURG

*Nordita, KTH Royal Institute of Technology and Stockholm University, 10691 Stockholm, Sweden;  
 JILA and Laboratory for Atmospheric and Space Physics, University of Colorado, Boulder, CO 80303, USA;  
 Department of Astronomy, Stockholm University, SE-10691 Stockholm, Sweden*

GUNILLA SVENSSON

*Department of Meteorology and Bolin Centre for Climate Research, Stockholm University, Stockholm, Sweden;  
 Swedish e-Science Research Centre, www.e-science.se, Stockholm, Sweden*

NILS E. L. HAUGEN

*SINTEF Energy Research, 7465 Trondheim, Norway;  
 Department of Energy and Process Engineering, NTNU, 7491 Trondheim, Norway*

BERNHARD MEHLIG

*Department of Physics, Gothenburg University, 41296 Gothenburg, Sweden*

IGOR ROGACHEVSKII

*Department of Mechanical Engineering, Ben-Gurion Univ. of the Negev, P. O. Box 653, Beer-Sheva 84105, Israel;  
 Nordita, KTH Royal Institute of Technology and Stockholm University, 10691 Stockholm, Sweden*

**ABSTRACT**

The effect of turbulence on combined condensational and collisional growth of cloud droplets is investigated using high-resolution direct numerical simulations. The motion of droplets is subjected to both turbulence and gravity. We solve the thermodynamic equations that govern the supersaturation field together with the hydrodynamic equations describing the turbulence. The collision-coalescence process is approximated by a superparticle approach assuming unit collision and coalescence efficiency, i.e., droplet coalesce upon collision. Condensational growth of cloud droplets due to supersaturation fluctuations depends on the Reynolds number, while the collisional growth was previously found to depend on the mean energy dissipation rate. Here we show that the combined processes depend on both Reynolds number and the mean energy dissipation rate. Droplet size distributions broaden either with increasing Reynolds number or mean energy dissipation rate in the range explored here. Even though collisional growth alone is insensitive to Reynolds number, it is indirectly affected by the large scales of turbulence through condensation. This is argued to be due to the fact that condensational growth results in wider droplet-size distributions, which triggers collisional growth. Since turbulence in warm clouds has a relatively small mean energy dissipation rate, but a large Reynolds number, turbulence mainly affects the condensational growth and thus influences the collisional growth indirectly through condensation. Thus, the combined condensational and collisional growth of cloud droplets is mostly dominated by Reynolds number. This work, for the first time, numerically demonstrates that supersaturation fluctuations enhance the collisional growth. It supports the findings from laboratory experiments and the observations that supersaturation fluctuations are important for precipitation.

## 1. Introduction

It has been suggested that warm rain accounts for about 30% of the total amount of rain and for 70% of the total rain area in the tropics, which plays an important role in regulating the vertical water and energy transport of the tropical atmosphere (Lau and Wu 2003). Its rapid formation has puzzled the cloud microphysics community for about 70 years. The observed time scale of warm rain formation is known to be about 20 minutes (Stephens and Haynes 2007), which is much shorter than the theoretically predicted time scale of 8 hours (Saffman and Turner 1956). Condensational and collisional growth determine the formation of warm rain. In the absence of turbulence, condensational growth is effective for cloud condensation nuclei and cloud droplets smaller than  $15\ \mu\text{m}$  in radius. Since the growth rate is inversely proportional to the radius, condensational growth leads to a narrow width of the droplet-size distribution. The gravity-generated collisional growth in isolation becomes important only when the mean radius of droplets is larger than  $\sim 40\ \mu\text{m}$ . Thus, there is a size gap of  $15\ \mu\text{m}$ – $40\ \mu\text{m}$  where neither condensation nor collision drives the growth (Pruppacher and Klett 2012; Lamb and Verlinde 2011; Grabowski and Wang 2013). Therefore, the effect of turbulence on condensational and collisional growth has been proposed to overcome this size gap (Saffman and Turner 1956; Shaw 2003; Devenish et al. 2012; Grabowski and Wang 2013). In the meteorology community, the process of collision-coalescence is also referred to as collection, while in the astrophysical community, this process is referred to as coagulation (Li et al. 2018a). Since we assume unit collision and coalescence efficiency, we use the terminology collision in the present study.

Saffman and Turner (1956) formulated the effect of turbulence on the collision rate in their pioneering work, referred to as the Saffman-Turner model. This model suggested that the collision rate is dominated by small scales of turbulence, because the typical size of cloud droplets (about  $10\ \mu\text{m}$  by radius) is about two orders of magnitude smaller than the Kolmogorov length (the smallest scale of turbulence, which is about 1 mm). Using dimensional analysis, Saffman and Turner (1956) predicted that the mean collision rate is proportional to the mean energy dissipation rate  $\bar{\epsilon}$  if there is no intermittency and if particle inertia is small. Following Saffman and Turner (1956), several stochastic models (Reuter et al. 1988; Grover and Pruppacher 1985; Pinsky and Khain 2004; Pinsky et al. 2007, 2008) suggested that turbulence causes a substantial enhancement of the collision rate. However,

Koziol and Leighton (1996) found that turbulence only has a moderate effect on the collision rate. Wang et al. (2005) and Grabowski and Wang (2013) argued that this discrepancy is either due to the simplified descriptions of the droplet motion or an inaccurate modelling of fluctuations in turbulence.

The rapid development of computers has made it feasible to study the condensational and collisional growth using direct numerical simulation (DNS). Most of the DNS studies of the collisional growth ignored the coalescence (Franklin et al. 2005; Ayala et al. 2008; Rosa et al. 2013; Chen et al. 2016; Woittiez et al. 2009), i.e., the size of the droplet does not change. This has helped to establish an understanding of the physical mechanisms that contribute to the collisional growth (Li et al. 2018a), such as turbulence enhancement on the relative velocity of droplets and droplet clustering, which were shown to be important to the collision rate (Shaw et al. 1998; Collins and Keswani 2004; Chun et al. 2005; Salazar et al. 2008; Bec et al. 2010; Gustavsson and Mehlig 2011, 2014; Ireland et al. 2016a,b; Meibohm et al. 2017). The turbulence effect on the geometric collision rate was investigated by Franklin et al. (2005), Ayala et al. (2008), Rosa et al. (2013), and Chen et al. (2016). They concluded that turbulence enhances the collision rate with increasing mean energy dissipation rate and that its dependency on the Reynolds number is secondary.

Franklin (2008), Xue et al. (2008), and Wang and Grabowski (2009) investigated the collision-coalescence processes by solving the Smoluchowski equation together with the Navier-Stokes equation using DNS. They found that the size distribution of cloud droplets is significantly enhanced by turbulence. Onishi and Seifert (2016) extended the collision-rate model of Wang and Grabowski (2009) and performed DNS at higher Reynolds number, where a Reynolds number dependency was obtained. Using a Lagrangian collision-detection method, Chen et al. (2018a) found that turbulence strongly affects the broadening of the size distribution. However, Li et al. (2018a) found that turbulence has a moderate effect on the collision-coalescence process and that the enhancement effect is sensitive to the initial width of droplet-size distributions. This finding turns out to be important for the present paper.

The effect of turbulence on condensational growth has also been explored intensively. Since turbulence affects the temperature field and spatial distribution of the water-vapor mixing ratio, the supersaturation field determined by temperature and water mixing ratio is inevitably affected by turbulence. Srivastava (1989) criticized the use of volume-averaged supersaturation and proposed adopting the local supersaturation field to calculate the condensational growth of cloud droplets. This is a prototype of supersaturation fluctuations. To investigate how supersaturation fluctuations affect the condensational

---

\* Corresponding author address: Xiang-Yu Li, Department of Meteorology and Bolin Centre for Climate Research, Stockholm University, Stockholm, Sweden  
E-mail: xiang.yu.li@su.se

growth, Vaillancourt et al. (2002) solved the thermodynamical equations that govern the supersaturation using DNS. They concluded that turbulence has a negligible effect on condensational growth. Paoli and Shariff (2009) investigated turbulence as well as the temperature and vapor fields and found that supersaturation fluctuations are responsible for the broadening of the droplet-size distribution, which is contrary to the findings by Vaillancourt et al. (2002). Lanotte et al. (2009), Sardina et al. (2015), and Siewert et al. (2017) conducted DNS for condensational growth by solving a passive scalar equation for the supersaturation and concluded that the size distribution broadens with increasing Reynolds number. Li et al. (2018b) investigated the effect of turbulence on condensational growth by solving the complete set of thermodynamic equations governing the supersaturation field and found that condensational growth strongly depends on the Reynolds number. Li et al. (2018b) suggested that the contradiction between the work of Vaillancourt et al. (2002) and the ones of others could be due to the fact that Vaillancourt et al. (2002) varied the Reynolds number and the mean energy dissipation rate at the same time. Also, the Reynolds number in Vaillancourt et al. (2002) is about three times smaller than in any of the other papers. Grabowski and Abade (2017) also found that the droplet-size distribution broadens due to supersaturation fluctuations by using a turbulent adiabatic parcel model.

Most of the previous DNS studies only considered either condensational growth or collisional growth. The combined condensational and collisional growth has rarely been investigated. Only recently, Saito and Gotoh (2017) studied the combined processes and found that the width of the droplet-size distribution increases with increasing turbulence intensity. However, they did not discuss which scales of turbulence matter for the broadening. Chen et al. (2018b) employed the same model as Saito and Gotoh (2017) and concluded that turbulence enhances the growth with increasing mean energy dissipation rate. However, they did not study the dependency of droplet-size distributions on Reynolds number. Indeed, several works (Lanotte et al. 2009; Sardina et al. 2015; Li et al. 2018b) suggested that condensational growth is sensitive to the Reynolds number. The collisional growth, however, is affected by the mean energy dissipation rate (Li et al. 2018a). To study the turbulence effect on the combined processes is challenging because both large and small scales of turbulence need to be well resolved. Saito and Gotoh (2017) and Chen et al. (2018b) also prescribed a mean updraft cooling in their work. They found that the mean updraft velocity of fluid parcels, mean supersaturation, and liquid-water content are all insensitive to the turbulence intensity.

In this paper, we investigate the effect of turbulence on the combined condensational and collisional growth of cloud droplets at different scales of turbulence using DNS.

The temperature field and the water-vapor mixing ratio field governing the supersaturation are advected by turbulence. Droplets, whose motion is subjected to turbulence and gravity are tracked in a Lagrangian manner. Their trajectories differs from those of gas flow tracers due to inertia. Droplets grow or shrink depending on the spatial and temporal variability of the local supersaturation. More importantly, the process of collision-coalescence is included, which is driven by both gravity and turbulence. Since we focus on the impact of turbulence on droplets growth, the mean updraft cooling is omitted. We first investigate how condensational and collisional processes affect each other through thermodynamics and droplet dynamics. Then, we explore how the combined condensational and collisional growth depends on the mean energy dissipation rate and the Reynolds number. We focus on the time evolution of the droplet-size distribution  $f(r, t)$ , which is one of the most important quantities in cloud microphysics since it is the key to the cloud-climate feedback and precipitation (Shaw 2003). The importance of our work lies in the fact that we are able to explain how condensation affects the collision. In earlier work of Chen et al. (2018b), condensational growth was thought to enhance the rate of collisions by producing a large number of similar-sized droplets as a consequence of a narrowing size distribution. Here, instead, we show that collisional growth is enhanced by the production of a broadening tail of the droplet-size distribution through supersaturation fluctuations.

## 2. Numerical model

In this section, the equations governing the Eulerian fields, droplet dynamics, condensation, and collisions are presented. They are solved using the PENCIL CODE; see Li et al. (2017) for an earlier application to droplet growth.

### a. Equations of motion for Eulerian fields

The background air flow is almost incompressible and is assumed to obey the Boussinesq approximation. This approximation assumes that density gradients are negligible except when multiplied by the gravitational acceleration, requiring temperature gradients to be small (see for example Mehaddi et al. (2018)). The density  $\rho(\mathbf{x}, t)$  is governed by the continuity equation while the velocity  $\mathbf{u}(\mathbf{x}, t)$  is obtained from the Navier-Stokes equation. The temperature  $T(\mathbf{x}, t)$  of the background air flow is determined by the energy equation with a source term due to the latent heat release. The water-vapor mixing ratio  $q_v(\mathbf{x}, t)$  is transported by the background air flow. Here,  $q_v(\mathbf{x}, t)$  is defined as the ratio between the mass density of water vapor and dry air. The Eulerian equations are given by

$$\frac{\partial \rho}{\partial t} + \nabla \cdot (\rho \mathbf{u}) = S_\rho, \quad (1)$$

$$\frac{Du}{Dt} = \mathbf{f} - \rho^{-1} \nabla p + \rho^{-1} \nabla \cdot (2\nu \rho \mathbf{S}) + B\mathbf{e}_z + \mathbf{S}_u, \quad (2)$$

$$\frac{DT}{Dt} = \kappa \nabla^2 T + \frac{L}{c_p} C_d, \quad (3)$$

$$\frac{Dq_v}{Dt} = D \nabla^2 q_v - C_d, \quad (4)$$

where  $D/Dt = \partial/\partial t + \mathbf{u} \cdot \nabla$  is the material derivative,  $\mathbf{f}$  is a random forcing function that is chosen to be the same as the one used in Haugen et al. (2004),  $\nu$  is the kinematic viscosity of air,  $S_{ij} = \frac{1}{2}(\partial_j u_i + \partial_i u_j) - \frac{1}{3} \delta_{ij} \nabla \cdot \mathbf{u}$  is the traceless rate-of-strain tensor,  $p$  is the gas pressure,  $\rho$  is the gas density,  $L$  is the latent heat,  $\kappa$  is the thermal diffusivity of air, and  $D$  is the water vapor diffusivity. In calculating the pressure, we ignore the heating and cooling processes and assume an adiabatic equation of state given by

$$p = \rho c_s^2 / \gamma, \quad (5)$$

where  $\gamma = c_p/c_v = 7/5$  (appropriate for diatomic gases such as air) is the ratio between specific heats at constant pressure and constant volume,  $c_p$  and  $c_v$ , respectively. We set the sound speed as  $5 \text{ m s}^{-1}$  to simulate the nearly incompressible atmospheric air flow, resulting in a Mach number of 0.06 when  $u_{\text{rms}} = 0.27 \text{ m s}^{-1}$ . Here  $u_{\text{rms}}$  is the rms velocity. Such a configuration, with so small Mach number, is equivalent to an incompressible flow. The source terms in equations 1 and 2 ( $S_p$  and  $\mathbf{S}_u$ ) come from the mass transfer between the droplets and the humid air due to condensation and evaporation, in addition to the one from the drag between the droplets and the air. However, since the mass transfer is small relative to the total mass of the air, and since the fraction of liquid to gaseous mass is also low, these terms are neglected in the remainder of this work. When solving the strict incompressible flow as in Vaillancourt et al. (2002) and Paoli and Shariff (2009), the source terms  $S_p$  and  $\mathbf{S}_u$  do not exist. The buoyancy  $B(\mathbf{x}, t)$  depends on the temperature  $T(\mathbf{x}, t)$ , upon the water-vapor mixing ratio  $q_v(\mathbf{x}, t)$ , and on the liquid-water mixing ratio  $q_l(\mathbf{x}, t)$  (Lamb and Verlinde 2011; Kumar et al. 2014),

$$B(\mathbf{x}, t) = g(T'/T + \alpha q'_v - q_l), \quad (6)$$

where  $\alpha = M_a/M_v - 1 \approx 0.608$  when  $M_a$  and  $M_v$  are the molar masses of air and water vapor, respectively. The amplitude of the gravitational acceleration is given by  $g$ . The liquid-water mixing ratio is the ratio between the mass density of liquid water and the dry air and is defined as (Lamb and Verlinde 2011; Li et al. 2018b),

$$q_l(\mathbf{x}, t) = \frac{4\pi\rho_l}{3\rho_a(\Delta x)^3} \sum_{j=1}^{N_\Delta} r^3(t) = \frac{4\pi\rho_l}{3\rho_a} \sum_{j=1}^{N_\Delta} f(r, \mathbf{x}, t) r^3(t) \delta r, \quad (7)$$

where  $\rho_l = 10^3 \text{ kg m}^{-3}$  and  $\rho_a = 1 \text{ kg m}^{-3}$  are the liquid-water density and the reference mass density of dry air.

$N_\Delta$  is the total number of droplets in a cubic grid cell with volume  $(\Delta x)^3$ , where  $\Delta x$  is the one-dimensional size of the grid box (Li et al. 2018b). The temperature fluctuations are defined as

$$T'(\mathbf{x}, t) = T(\mathbf{x}, t) - T_{\text{env}}, \quad (8)$$

and the water-vapor mixing ratio fluctuations by

$$q'_v(\mathbf{x}, t) = q_v(\mathbf{x}, t) - q_{v, \text{env}}, \quad (9)$$

where the mean environmental temperature  $T_{\text{env}}$  and water-vapor mixing ratio  $q_{v, \text{env}}$  are constant. The condensation rate  $C_d$  is given by (Vaillancourt et al. 2001)

$$\begin{aligned} C_d(\mathbf{x}, t) &= \frac{4\pi\rho_l G}{\rho_a(\Delta x)^3} \sum_{j=1}^{N_\Delta} s(\mathbf{x}, t) r(t) \\ &= \frac{4\pi\rho_l G}{\rho_a} \sum_{j=1}^{N_\Delta} s(\mathbf{x}, t) f(r, \mathbf{x}, t) r(t) \delta r, \end{aligned} \quad (10)$$

where  $G$  is the condensation parameter that varies slowly with temperature and pressure (Lamb and Verlinde 2011) and is thus assumed to be constant (having units of  $\text{m}^2 \text{ s}^{-1}$ ). The supersaturation  $s$  is defined as

$$s(\mathbf{x}, t) = \frac{q_v(\mathbf{x}, t)}{q_{vs}(T)} - 1, \quad (11)$$

and  $q_{vs}(T)$  is the saturation water vapor mixing ratio at temperature  $T$  and can be determined via the ideal gas law,

$$q_{vs}(T) = \frac{e_s(T)}{R_v \rho_0 T}. \quad (12)$$

The saturation pressure  $e_s$  is determined via the Clausius-Clapeyron equation (Yau and Rogers 1996; Götzfried et al. 2017),

$$e_s(T) = c_1 \exp(-c_2/T), \quad (13)$$

where  $c_1$  and  $c_2$  are constants. We refer to Table 1 for all the thermodynamics constants and Li et al. (2018b) for details of the numerical setup.

#### b. Lagrangian model for dynamics of cloud droplets

We approximate the droplet dynamics using a stochastic Monte Carlo algorithm (Bird 1978, 1981; Jorgensen et al. 1983) that represents a number of spherical droplets by a superparticle (Zsom and Dullemond 2008; Shima et al. 2009; Johansen et al. 2012; Li et al. 2017, 2018a). All droplets in superparticle  $i$  are assumed to have the same material density  $\rho_l$ , radius  $r_i$ , and velocity  $\mathbf{v}_i$ . Further, each superparticle is assigned a volume of the grid cell and thus a droplet number density,  $n_i$ . Each superdroplet is treated

as a Lagrangian point-particle, where one solves for the particle position  $\mathbf{x}_i$ ,

$$\frac{d\mathbf{x}_i}{dt} = \mathbf{V}_i, \quad (14)$$

and its velocity  $\mathbf{V}_i$  via

$$\frac{d\mathbf{V}_i}{dt} = \frac{1}{\tau_i}(\mathbf{u} - \mathbf{V}_i) + \mathbf{g} \quad (15)$$

in the usual way; see Li et al. (2017) for details. Here,  $\mathbf{u}$  is the fluid velocity at the position of the droplet,  $\mathbf{g}$  is the gravitational acceleration,  $\tau_i$  is the inertial response (or stopping) time of a droplet  $i$  and is given by

$$\tau_i = 2\rho_l r_i^2 / [9\rho v D(\text{Re}_i)]. \quad (16)$$

The correction factor (Schiller and Naumann 1933; Marchioli et al. 2008)

$$D(\text{Re}_i) = 1 + 0.15 \text{Re}_i^{2/3} \quad (17)$$

is used to approximate the effect of non-zero particle Reynolds number  $\text{Re}_i = 2r_i|\mathbf{u} - \mathbf{V}_i|/\nu$ .

#### c. Condensation and collisions of Lagrangian droplets

The condensational growth of droplets is governed by (Pruppacher and Klett 2012; Lamb and Verlinde 2011),

$$\frac{dr_i}{dt} = \frac{Gs(\mathbf{x}_i, t)}{r_i}. \quad (18)$$

Collisional growth of cloud droplets is modeled by using a superparticle approach (Shima et al. 2009; Johansen et al. 2012; Li et al. 2017, 2018a). When two superparticles reside in the same grid cell, the probability of collision between one droplet in a superparticle colliding with droplets in another superparticle is  $p_c = \tau_c^{-1} \Delta t$ , where  $\Delta t$  is the integration time step. A collision event only occurs when  $p_c > \eta_c$ , where  $\eta_c$  is a random number between zero and one (Li et al. 2018a). The collision time  $\tau_c$  is determined by

$$\tau_c^{-1} = \sigma_c n_j |\mathbf{V}_i - \mathbf{V}_j| E_c. \quad (19)$$

Here  $\sigma_c = \pi(r_i + r_j)^2$  is the geometric collision cross-section between two droplets with radii  $r_i$  and  $r_j$ . The parameter  $E_c$  is the collision efficiency, which is set to unity for simplicity. We refer to Li et al. (2017) and Li et al. (2018a) for details of the algorithm.

#### d. Initial conditions

We use the same initial configuration as in Li et al. (2018b) where the initial values (see Table 1) of the water-vapor mixing ratio are  $q_v(\mathbf{x}, t = 0) = 0.0157 \text{ kg} \cdot \text{kg}^{-1}$  and

TABLE 1. List of constants for the thermodynamics: see text for explanations of symbols.

Quantity	Value
$\nu$ ( $\text{m}^2 \text{s}^{-1}$ )	$1.5 \times 10^{-5}$
$\kappa$ ( $\text{m}^2 \text{s}^{-1}$ )	$1.5 \times 10^{-5}$
$D$ ( $\text{m}^2 \text{s}^{-1}$ )	$2.55 \times 10^{-5}$
$G$ ( $\text{m}^2 \text{s}^{-1}$ )	$1.17 \times 10^{-10}$
$c_1$ (Pa)	$2.53 \times 10^{11}$
$c_2$ (K)	5420
$L$ ( $\text{J} \cdot \text{kg}^{-1}$ )	$2.5 \times 10^6$
$c_p$ ( $\text{J} \cdot \text{kg}^{-1} \text{K}^{-1}$ )	1005.0
$R_v$ ( $\text{J} \cdot \text{kg}^{-1} \text{K}^{-1}$ )	461.5
$M_a$ ( $\text{g} \cdot \text{mol}^{-1}$ )	28.97
$M_v$ ( $\text{g} \cdot \text{mol}^{-1}$ )	18.02
$\alpha$	0.608
$\rho_a$ ( $\text{kg} \cdot \text{m}^{-3}$ )	1
$\rho_l$ ( $\text{kg} \cdot \text{m}^{-3}$ )	1000
$Pr = \nu/\kappa$	1
$Sc = \nu/D$	0.6
$q_v(\mathbf{x}, t = 0)$ ( $\text{kg} \cdot \text{kg}^{-1}$ )	0.0157
$q_{v, \text{env}}$ ( $\text{kg} \cdot \text{kg}^{-1}$ )	0.01
$T(\mathbf{x}, t = 0)$ (K)	292
$T_{\text{env}}$ (K)	293

temperature  $T(\mathbf{x}, t = 0) = 292 \text{ K}$  respectively. This provides an initially saturated environment. The time step of the simulations presented here is governed by the smallest time scale in the current configuration, which is the collision time scale of the colliding droplet pairs. The thermodynamic and Kolmogorov time scales are larger than the collision time scale.

Initially, 10  $\mu\text{m}$ -sized (by radius) droplets with zero velocity are randomly distributed in the simulation domain. The initial mean number density of droplets is  $n_0 = 2.5 \times 10^8 \text{ m}^{-3}$ . This gives an initial liquid-water content,  $(4\pi\rho_l/3) \int_0^\infty f(r, t = 0) r^3 dr$ , which is  $0.001 \text{ kg m}^{-3}$ . The simulation domain is a cube of size  $L_x = L_y = L_z$ , the values of which are given in Table 2. The number of superdroplets  $N_s$  satisfies  $N_s/N_{\text{grid}} \approx 0.1$ , where  $N_{\text{grid}}$  is the number of lattices depending on the spatial resolution of the simulations. Setting  $N_s/N_{\text{grid}} \approx 0.1$ , on the one hand, is still within the convergence range  $N_s/N_{\text{grid}} \approx 0.05$  (Li et al. 2018b). On the other hand, it can mimic the diluteness of the atmospheric cloud system, which has about 0.1 droplets per cubic Kolmogorov length scale.

#### e. DNS

Three types of simulations are performed: condensational growth, collisional growth, combined condensational and collisional growth. We investigated the effect of

turbulence on condensational growth in Li et al. (2018b) and collisional growth in Li et al. (2018a). Here, we take one simulation for condensational growth and one for collisional growth as references. We conduct high resolution simulations for different Taylor micro-scale Reynolds number  $Re_\lambda$  and mean energy dissipation rate  $\bar{\epsilon}$  (see Table 2 for details of the simulations) for combined condensational and collisional growth. The Taylor micro-scale Reynolds number is defined as  $Re_\lambda \equiv u_{rms}^2 \sqrt{5/(3\nu\bar{\epsilon})}$ . For simulations with different values of  $\bar{\epsilon}$  at fixed  $Re_\lambda$ , we vary both the domain size  $L_x$  ( $L_y = L_z = L_x$ ) and the amplitude of the forcing  $f_0$ . As for fixed  $\bar{\epsilon}$ ,  $Re_\lambda$  is varied by solely changing the domain size, which in turn changes  $u_{rms}$ . In all simulations, we use for the Prandtl number  $Pr = \nu/\kappa = 1$  and for the Schmidt number  $Sc = \nu/D = 0.6$ , which are the same values as those used in Li et al. (2018b).

### 3. Results

#### a. Comparison between the three different cases: condensational growth, collisional growth, and the combined case

Condensational growth of cloud droplets is subjected to supersaturation fluctuations (Lanotte et al. 2009; Sardina et al. 2015; Grabowski and Abade 2017; Li et al. 2018b), which are determined by  $T(\mathbf{x}, t)$  and  $q_v(\mathbf{x}, t)$ . We first investigate how collision impacts these field quantities and therefore, the condensational growth. Figure 1 shows the time series of  $T_{rms}(t)$ ,  $q_{v,rms}(t)$ ,  $B_{rms}(t)$ ,  $s_{rms}(t)$ ,  $q_{l,rms}(t)$ , and  $C_{d,rms}(t)$  with or without collisions. We see that the collisional process does not affect fluctuations of most of these quantities except for  $B_{rms}(t)$  and  $q_{l,rms}(t)$ . The buoyancy force  $B$  is determined by temperature fluctuations  $T'$ , water-vapor mixing ratio fluctuations  $q'_v$ , and liquid-water mixing ratio  $q_l$ . The collision process leads to more intense local variations of  $q_l$ , which results in larger  $q_{l,rms}$ . Therefore,  $B_{rms}(t)$  is enhanced by the collision process through  $q_l$ . The enhanced  $B$ , however, does not affect the flow field since the random forcing dramatically overwhelms the buoyancy force in our simulations. Thus, collisional growth does not impact the condensational growth in the present DNS.

Next, we investigate how condensational growth affects the collisional growth by comparing the time evolution of the droplet-size distribution for three different cases: condensation only, collision only, and the combined process. Figure 2(a) shows the comparison of droplet-size distributions when  $Re_\lambda = 45$  and  $\bar{\epsilon} = 0.039 \text{ m}^2 \text{ s}^{-3}$ . For the case with only condensation, the growth leads to a broadening of the size distribution. When comparing the tail of the size distribution between the cases of collision only and that of the combined process, we see that the broadening from the condensational growth facilitates the collisional growth. The combined condensational and collisional growth leads to the largest tail of the size distribution.

At  $t = 80 \text{ s}$ , the largest radius resulting from the case of combined condensation and collision is about  $27.4 \mu\text{m}$  and the one resulting from the case of collision only is about  $26.7 \mu\text{m}$ . This leads to an increased rate of  $27.4/26.7 - 1 \approx 3\%$ . When  $Re_\lambda = 130$  and  $\bar{\epsilon} = 0.039 \text{ m}^2 \text{ s}^{-3}$ , the rate increases to  $32.3/29.3 - 1 \approx 10\%$ , as shown in Figure 2(b). It is worth noting that for the combined process, the droplet-size distribution exhibits an obvious transition from condensational growth to collisional growth, as shown by the dip in the droplet-size distribution. We recall that the radii of all droplets are initially  $10 \mu\text{m}$ . After the first collision, the droplet grows to twice the mass, giving a radius of  $12.6 \mu\text{m}$ . Condensational growth leads to a few large droplets (close to  $12.6 \mu\text{m}$  by radius) from the initially monodispersed  $10 \mu\text{m}$  droplet distribution, which triggers the collision process. For the case of  $Re_\lambda = 130$  (cyan curves), the dips are less abrupt. This is due to the fact that larger  $Re_\lambda$  leads to stronger supersaturation fluctuations, thus, generate more large droplets.

The collisional growth of cloud droplets is very sensitive to the tails of droplet-size distributions. A few large droplets can undergo a runaway collision-coalescence process by collecting small droplets. The cumulative collision time of these few large droplets is much shorter than the mean collision time (Kostinski and Shaw 2005). Thus, fluctuations play an important role in collisional growth. Condensational growth due to supersaturation fluctuations facilitates this runaway collision process by generating the few large droplets.

#### b. Effect of turbulence on combined condensational and collisional growth

To study the effect of turbulence on the combined condensational and collisional growth, we explore how the time evolution of droplet-size distributions depend on  $\bar{\epsilon}$  and  $Re_\lambda$  when the growth of droplet is driven by both condensation and collision. Our previous work (Li et al. 2018b) showed that condensational growth is enhanced with increasing  $Re_\lambda$  but is insensitive to  $\bar{\epsilon}$ . Collisional growth, however, weakly depends on  $\bar{\epsilon}$  and is insensitive to  $Re_\lambda$  (Li et al. 2018a). Therefore, we expect that the combined condensational and collisional growth depends on both  $Re_\lambda$  and  $\bar{\epsilon}$ . Figure 3(a) shows the time evolution of droplet-size distributions for different  $\bar{\epsilon}$  with fixed  $Re_\lambda$ . The first peak and its width are almost the same for different  $\bar{\epsilon}$  at different times, which exhibits the same characters as the simulations without collisions in Li et al. (2018b). We attribute this feature to condensational growth and its weak dependency on  $\bar{\epsilon}$ . The tail of the droplet-size distribution becomes wider with increasing  $\bar{\epsilon}$ , which is attributed to the dependency of collisional growth on  $\bar{\epsilon}$ . Comparing the largest radius for the case of  $\bar{\epsilon} = 0.005 \text{ m}^2 \text{ s}^{-3}$  and the case of  $\bar{\epsilon} = 0.039 \text{ m}^2 \text{ s}^{-3}$  at  $t = 80 \text{ s}$ , we find that the largest radius increases by

TABLE 2. Summary of the simulations.

Run	$f_0$	$L_x$ (m)	$N_{\text{grid}}$	$N_s$	Processes	$u_{\text{rms}}$ (ms <sup>-1</sup> )	$\text{Re}_\lambda$	$\bar{\epsilon}$ (m <sup>2</sup> s <sup>-3</sup> )	$\eta \cdot 10^{-4}$ (m)	$\tau_\eta$ (s)	$\tau_L$ (s)
A	0.007	0.200	$128^3$	$N_{s,128}$	Both	0.10	44	0.005	9.2	0.056	0.67
B	0.014	0.150	$128^3$	$N_{s,128}$	Both	0.14	45	0.019	6.5	0.028	0.35
C	0.020	0.125	$128^3$	$N_{s,128}$	Both	0.16	45	0.039	5.4	0.020	0.25
C1	0.020	0.125	$128^3$	$N_{s,128}$	Con	0.16	45	0.039	5.4	0.020	0.25
C2	0.020	0.125	$128^3$	$N_{s,128}$	Col	0.16	45	0.039	5.4	0.020	0.25
D	0.020	0.250	$256^3$	$2^3 N_{s,128}$	Both	0.22	78	0.039	5.4	0.020	0.37
E	0.020	0.500	$512^3$	$2^6 N_{s,128}$	Both	0.28	130	0.039	5.4	0.020	0.58
E1	0.020	0.500	$512^3$	$2^6 N_{s,128}$	Con	0.28	130	0.039	5.4	0.020	0.58
E2	0.020	0.500	$512^3$	$2^6 N_{s,128}$	Col	0.28	130	0.039	5.4	0.020	0.58

“Con” refers to condensation; “Col” refers to collision; “Both” refers to condensation and collision.

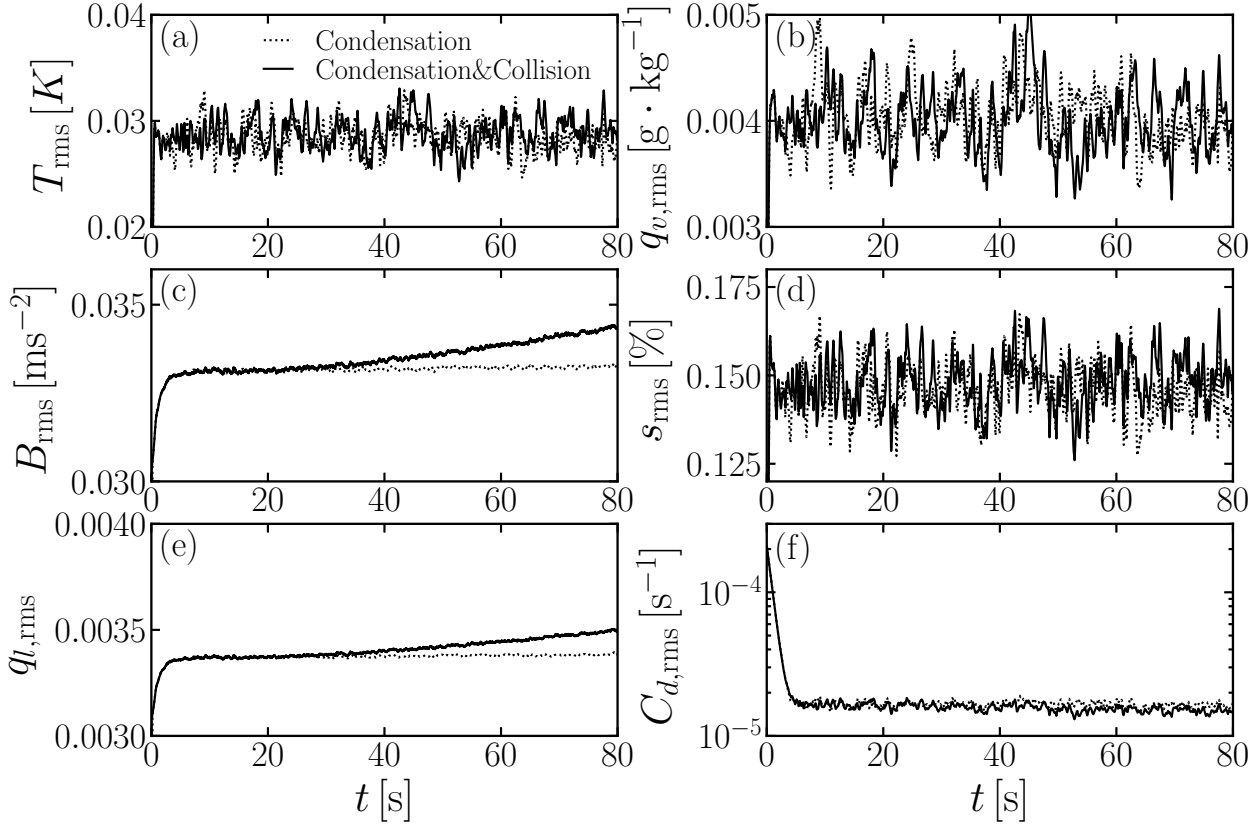


FIG. 1. Time series of (a)  $T_{\text{rms}}$ ; (b)  $q_{v,\text{rms}}$ ; (c)  $B_{\text{rms}}$ ; (d)  $s_{\text{rms}}$ ; (e)  $q_{t,\text{rms}}$ ; and (f)  $C_{d,\text{rms}}$ . Black dotted line: condensation only; black solid line: condensation and collision (see Runs C and C1 in Table 2 for details of the numerical setup).

$27/22 - 1 \approx 23\%$ . Figure 3(b), on the other hand, shows time evolution of droplet-size distributions for different  $\text{Re}_\lambda$  with fixed  $\bar{\epsilon}$ . The first peaks exhibit the same shape and dependency on  $\text{Re}_\lambda$  as the ones when collision was not included (Li et al. 2018b). The distributions of small droplets becomes wider with increasing  $\text{Re}_\lambda$ , which is due to the fact that condensational growth is enhanced with

increasing  $\text{Re}_\lambda$ . The tail of the droplet-size distribution broadens with increasing  $\text{Re}_\lambda$ . This is attributed to the condensational growth and its induced collision since collisional growth only depends on  $\bar{\epsilon}$ . We again check the largest radius for the case of  $\text{Re}_\lambda = 45$  and  $\text{Re}_\lambda = 130$ . The increased rate of the largest radius is  $32.3/27.4 - 1 \approx 20\%$ .

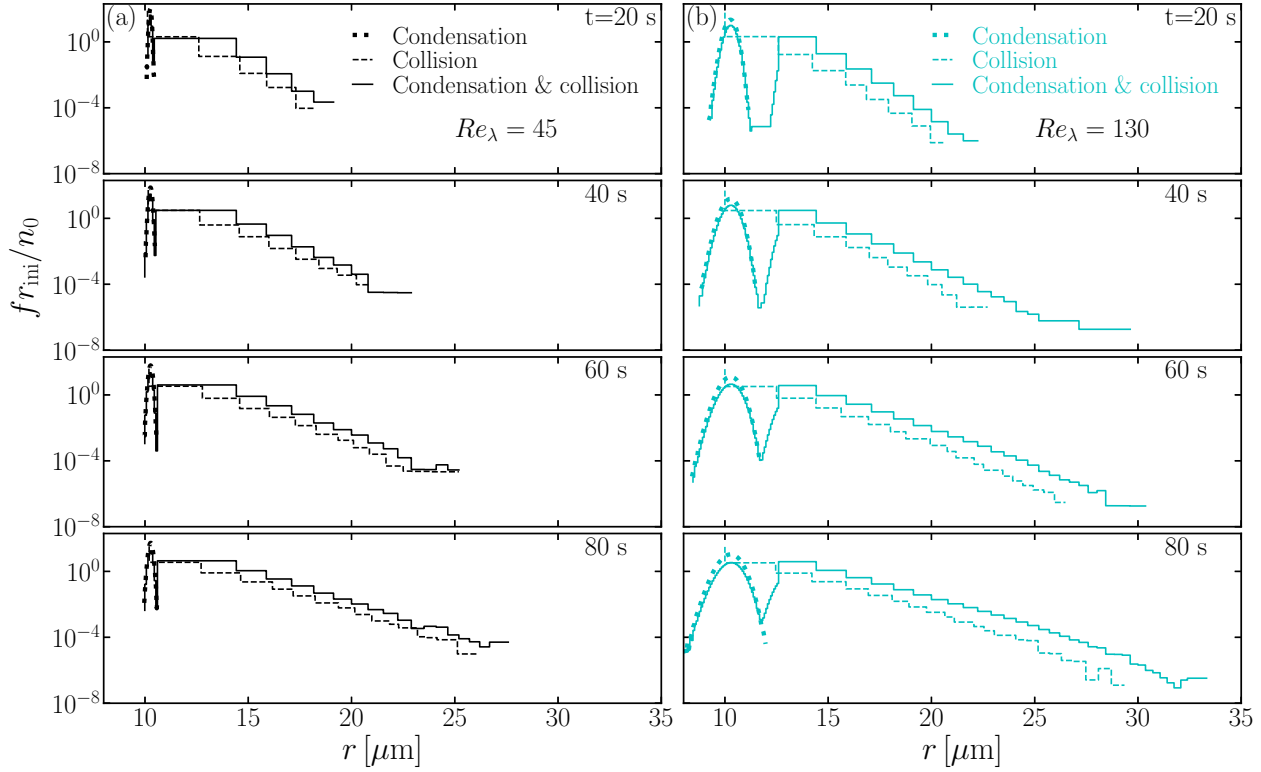


FIG. 2. Comparison of droplet-size distributions for three cases: condensational growth (dotted lines), collisional growth (dashed lines), and the combined processes (solid lines); see Runs C, C1, C2, E, E1, and E2 in Table 2 for details of the numerical setup. (a)  $Re_\lambda = 45$ ; (b)  $Re_\lambda = 130$ .

#### 4. Conclusions

We first investigated how the condensation process and collision process affect each other by comparing droplet-size distributions for three cases: pure condensation, pure collision, and the combined processes. We found that condensational growth broadens the droplet-size distributions in the initial phase of droplet growth, after which collisional growth is triggered. The condensation-triggered collision is pronounced with larger  $Re_\lambda = 130$ . The collision process only enhances the buoyancy force and does not affect the temperature, water-vapor mixing ratio, and supersaturation. Therefore, it does not influence the condensation process.

Next, we studied the combined condensational and collisional growth at different  $\bar{\epsilon}$  and  $Re_\lambda$ . We observed that the droplet-size distribution broadens with either increasing  $\bar{\epsilon}$  or  $Re_\lambda$ . The dependency on  $Re_\lambda$  can be explained as follows. Our previous studies (Li et al. 2018a) showed that collisional growth weakly depends on  $\bar{\epsilon}$  and is insensitive to  $Re_\lambda$ . The condensational growth, instead, strongly depends on  $Re_\lambda$  and is insensitive to  $\bar{\epsilon}$  (Li et al. 2018b). Also, in the present study, the comparison among cases of pure condensation, pure collision, and the combined process demonstrates that condensational growth triggers the

collisional growth. Therefore, we conclude that the  $Re_\lambda$  dependency is caused by the condensation process, which indirectly enhances the collisional growth. The combined processes are also observed to depend on  $\bar{\epsilon}$ , which is attributed to the dependency of the collisional growth on  $\bar{\epsilon}$ . However, the largest  $\bar{\epsilon}$  in warm clouds is only about  $\bar{\epsilon} = 10^{-3} \text{ m}^2 \text{ s}^{-3}$  (Siebert et al. 2006), so its effect on collisional growth is small (Li et al. 2018a). In reality, we have  $Re_\lambda \approx 10^4$  in a cloud system. It is expected that a higher  $Re_\lambda$  would lead to larger supersaturation fluctuations, and therefore fast broadening of the size distribution, which facilitates the collisional growth. Our findings also support results of the laboratory experiment of Chandrakar et al. (2016) that supersaturation fluctuations are likely of leading importance for precipitation formation. Furthermore, we demonstrated numerically that supersaturation fluctuations enhance the collisional growth.

In conclusion, we have found that the large scales of turbulence have a substantial effect on the growth of cloud droplets in warm clouds. Here the large scales represent the turbulent scales that are larger than the Kolmogorov scale and smaller than the turbulence integral scale. The condensational growth is driven by supersaturation fluctuations. Supersaturation fluctuations are governed by fluc-



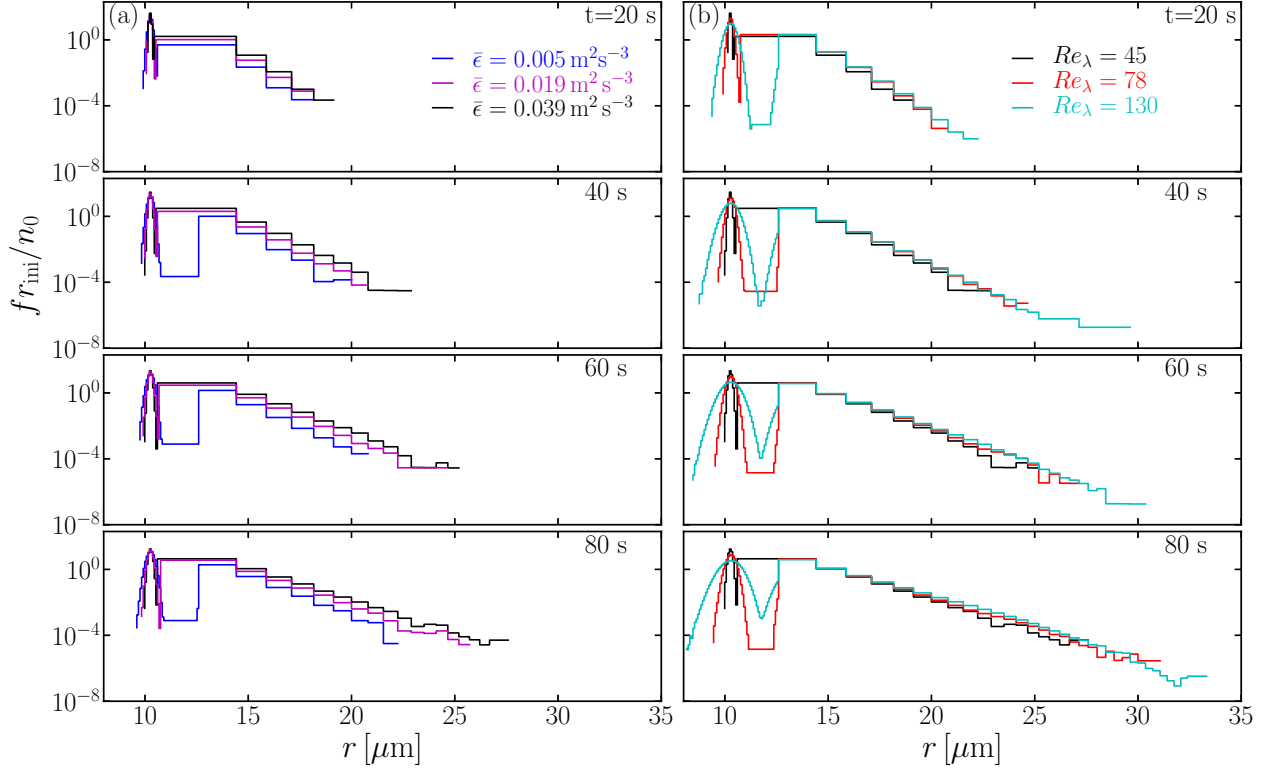


FIG. 3. Droplet size distributions for (a) different  $\bar{\epsilon} = 0.005 \text{ m}^2 \text{ s}^{-3}$  (blue solid lines), 0.019 (magenta solid lines) and 0.039 (black solid line) at fixed  $Re_\lambda = 45$  (see Runs A, B, and C in Table 2 for details) and for (b) different  $Re_\lambda = 45$  (black solid lines), 78 (red solid lines), and 130 (cyan solid line) at fixed  $\bar{\epsilon} = 0.039 \text{ m}^2 \text{ s}^{-3}$  (see Runs C, D, and E in Table 2 for details).

tuations of temperature and the water-vapor mixing ratio, which were found to be affected by the large scales of turbulence (Li et al. 2018b). After the droplet-size distribution has reached a certain width, collisional growth starts to dominate the growth, which is then weakly affected by the small scales of turbulence. Thus, large scales of turbulence influence the collisional growth indirectly through condensation. Small scales of turbulence affect both condensational and collisional growth weakly. Therefore, the combined condensational and collisional growth is influenced by turbulence from large to small scales.

Chen et al. (2018b) compared droplet size distributions for different  $\bar{\epsilon}$  when both condensation and collision were considered. They attributed the condensation-induced collision to the fact that “*condensational growth narrows the droplet size distribution (DSD) and provides a great number of similar-sized droplets*” (Chen et al. 2018b), which is inconsistent with our finding that condensational growth produces wider distributions with increasing  $Re_\lambda$  and therefore facilitates the collisional growth. We scrutinized the turbulence effect on condensational growth and found that the droplet size distribution shrinks slightly with increasing  $\bar{\epsilon}$  and increases strongly with increasing  $Re_\lambda$

(Li et al. 2018b). Therefore, the discrepancy between the present results and those of Chen et al. (2018b) could be due to the fact that, in their simulations,  $Re_\lambda$  and  $\bar{\epsilon}$  were changed at the same time.

As discussed at the end of Section a, our study lends some support to the notion of “lucky” droplets (Kostinski and Shaw 2005), first proposed by Telford (1955). The lucky-droplet model assumes that there is a larger droplet amongst many small ones to initiate the runaway growth (Kostinski and Shaw 2005; Wilkinson 2016). The question is where the first few lucky droplets come from. Kostinski and Shaw (2005) proposed that the first few lucky droplets could be the result of giant condensation nuclei. The present study indicates that the first few lucky droplets could result from condensational growth driven by supersaturation fluctuations caused by turbulence.

In the present study, the collision efficiency was assumed to be unity, which may substantially overestimate the collisional growth. Since turbulence-induced collision efficiency is a very challenging problem (Grabowski and Wang 2013), we seek to incorporate a parameterization-free scheme of collision efficiency in

the current superparticle approach. Entrainment is also omitted, which is supposed to cause strong supersaturation fluctuations. Aerosol activation is not included in the present study. Invoking all the cloud microphysical processes is computationally extremely demanding even on modern supercomputers. We strive to achieve this in future studies. Therefore, due to these limitations, we have not attempted to compare droplet-size distributions obtained from the current work with observational data.

## Acknowledgements

This work was supported through the FRINATEK grant 231444 under the Research Council of Norway, SeRC, the Swedish Research Council grants 2012-5797 and 2013-03992, the University of Colorado through its support of the George Ellery Hale visiting faculty appointment, the grant “Bottlenecks for particle growth in turbulent aerosols” from the Knut and Alice Wallenberg Foundation, Dnr. KAW 2014.0048, and Vetenskapsrådet with grant number 017-03865 and 2014-585. The simulations were performed using resources provided by the Swedish National Infrastructure for Computing (SNIC) at the Royal Institute of Technology in Stockholm and Chalmers Centre for Computational Science and Engineering (C3SE). This work also benefited from computer resources made available through the Norwegian NOTUR program, under award NN9405K. The source code used for the simulations of this study, the PENCIL CODE, is freely available on <https://github.com/pencil-code/>.

## References

- Ayala, O., B. Rosa, and L.-P. Wang, 2008: Effects of turbulence on the geometric collision rate of sedimenting droplets. part 2. theory and parameterization. *New J. Phys.*, **10** (9), 099 802.
- Bec, J., L. Biferale, M. Cencini, A. Lanotte, and F. Toschi, 2010: Intermittency in the velocity distribution of heavy particles in turbulence. *Journal of Fluid Mechanics*, **646**, 527–536.
- Bird, G., 1978: Monte carlo simulation of gas flows. *Annu. Rev. Fluid Mech.*, **10** (1), 11–31.
- Bird, G., 1981: Monte-carlo simulation in an engineering context. *Progress in Astronautics and Aeronautics*, **74**, 239–255.
- Chandrakar, K. K., W. Cantrell, K. Chang, D. Ciochetto, D. Niedermeier, M. Ovchinnikov, R. A. Shaw, and F. Yang, 2016: Aerosol indirect effect from turbulence-induced broadening of cloud-droplet size distributions. *Proceedings of the National Academy of Sciences*, **113** (50), 14 243–14 248.
- Chen, S., P. Bartello, M. Yau, P. Vaillancourt, and K. Zwijssen, 2016: Cloud droplet collisions in turbulent environment: Collision statistics and parameterization. *J. Atmosph. Sci.*, **73** (2), 621–636.
- Chen, S., M. Yau, and P. Bartello, 2018a: Turbulence effects of collision efficiency and broadening of droplet size distribution in cumulus clouds. *J. Atmosph. Sci.*, **75** (1), 203–217.
- Chen, S., M.-K. Yau, P. Bartello, and L. Xue, 2018b: Bridging the condensation–collision size gap: a direct numerical simulation of continuous droplet growth in turbulent clouds. *Atmospheric Chemistry and Physics*, **18** (10), 7251–7262.
- Chun, J., D. L. Koch, S. L. Rani, A. Ahluwalia, and L. R. Collins, 2005: Clustering of aerosol particles in isotropic turbulence. *J. Fluid Mech.*, **536**, 219–251.
- Collins, L. R., and A. Keswani, 2004: Reynolds number scaling of particle clustering in turbulent aerosols. *New J. Phys.*, **6** (1), 119.
- Devenish, B., and Coauthors, 2012: Droplet growth in warm turbulent clouds. *Quart. J. Roy. Meteorol. Soc.*, **138** (667), 1401–1429.
- Franklin, C. N., 2008: A warm rain microphysics parameterization that includes the effect of turbulence. *J. Atmosph. Sci.*, **65** (6), 1795–1816.
- Franklin, C. N., P. A. Vaillancourt, M. Yau, and P. Bartello, 2005: Collision rates of cloud droplets in turbulent flow. *J. Atmosph. Sci.*, **62** (7), 2451–2466.
- Götzfried, P., B. Kumar, R. A. Shaw, and J. Schumacher, 2017: Droplet dynamics and fine-scale structure in a shearless turbulent mixing layer with phase changes. *Journal of Fluid Mechanics*, **814**, 452–483.
- Grabowski, W. W., and G. C. Abade, 2017: Broadening of cloud droplet spectra through eddy hopping: Turbulent adiabatic parcel simulations. *Journal of the Atmospheric Sciences*, **74** (5), 1485–1493.
- Grabowski, W. W., and L.-P. Wang, 2013: Growth of cloud droplets in a turbulent environment. *Annu. Rev. Fluid Mech.*, **45** (1), 293–324, <http://dx.doi.org/10.1146/annurev-fluid-011212-140750>.
- Grover, S., and H. Pruppacher, 1985: The effect of vertical turbulent fluctuations in the atmosphere on the collection of aerosol particles by cloud drops. *J. Atmosph. Sci.*, **42** (21), 2305–2318.
- Gustavsson, K., and B. Mehlig, 2011: Distribution of relative velocities in turbulent aerosols. *Physical Review E*, **84** (4), 045 304.
- Gustavsson, K., and B. Mehlig, 2014: Relative velocities of inertial particles in turbulent aerosols. *Journal of Turbulence*, **15** (1), 34–69.
- Haugen, N. E. L., A. Brandenburg, and W. Dobler, 2004: Simulations of nonhelical hydromagnetic turbulence. *Phys. Rev. E*, **70** (1), 016308, doi:10.1103/PhysRevE.70.016308, astro-ph/0307059.
- Ireland, P. J., A. D. Bragg, and L. R. Collins, 2016a: The effect of reynolds number on inertial particle dynamics in isotropic turbulence. part 1. simulations without gravitational effects. *J. Fluid Mech.*, **796**, 617–658.
- Ireland, P. J., A. D. Bragg, and L. R. Collins, 2016b: The effect of reynolds number on inertial particle dynamics in isotropic turbulence. part2. simulations with gravitational effects. *J. Fluid Mech.*, **796**, 659–711.
- Johansen, A., A. N. Youdin, and Y. Lithwick, 2012: Adding particle collisions to the formation of asteroids and kuiper belt objects via streaming instabilities. *Astron. Astroph.*, **537**, A125.
- Jorgensen, W. L., J. Chandrasekhar, J. D. Madura, R. W. Impey, and M. L. Klein, 1983: Comparison of simple potential functions for simulating liquid water. *J. Chem. Phys.*, **79** (2), 926–935.
- Kostinski, A. B., and R. A. Shaw, 2005: Fluctuations and luck in droplet growth by coalescence. *Bull. Am. Met. Soc.*, **86**, 235–244.

- Koziol, A. S., and H. Leighton, 1996: The effect of turbulence on the collision rates of small cloud drops. *J. Atmosph. Sci.*, **53** (13), 1910–1920.
- Kumar, B., J. Schumacher, and R. A. Shaw, 2014: Lagrangian mixing dynamics at the cloudy-clear air interface. *Journal of the Atmospheric Sciences*, **71** (7), 2564–2580, doi:10.1175/JAS-D-13-0294.1, URL <http://dx.doi.org/10.1175/JAS-D-13-0294.1>, <http://dx.doi.org/10.1175/JAS-D-13-0294.1>.
- Lamb, D., and J. Verlinde, 2011: *Physics and Chemistry of Clouds*. Cambridge, England, Cambridge Univ. Press.
- Lanotte, A. S., A. Seminara, and F. Toschi, 2009: Cloud droplet growth by condensation in homogeneous isotropic turbulence. *Journal of the Atmospheric Sciences*, **66** (6), 1685–1697, doi:10.1175/2008JAS2864.1, URL <http://dx.doi.org/10.1175/2008JAS2864.1>, <http://dx.doi.org/10.1175/2008JAS2864.1>.
- Lau, K., and H. Wu, 2003: Warm rain processes over tropical oceans and climate implications. *Geophysical Research Letters*, **30** (24).
- Li, X.-Y., A. Brandenburg, N. Haugen, B. Mehlig, I. Rogachevskii, and G. Svensson, 2018a: Effect of turbulence on collisional growth of cloud droplets. *J. Atmosph. Sci.*, in press, arXiv:1711.10062.
- Li, X.-Y., A. Brandenburg, N. E. L. Haugen, and G. Svensson, 2017: Eulerian and Lagrangian approaches to multidimensional condensation and collection. *Journal of Advances in Modeling Earth Systems*, **9** (2), 1116–1137.
- Li, X.-Y., G. Svensson, A. Brandenburg, and N. E. Haugen, 2018b: Cloud droplets growth due to supersaturation fluctuations in stratiform clouds. *arXiv preprint arXiv:1806.10529*.
- Marchioli, C., and Coauthors, 2008: Statistics of particle dispersion in direct numerical simulations of wall-bounded turbulence: Results of an international collaborative benchmark test. *Intern. J. Multiphase Flow*, **34** (9), 879–893.
- Mehaddi, R., F. Candelier, and B. Mehlig, 2018: Inertial drag on a sphere settling in a stratified fluid. *arXiv preprint arXiv:1802.10416*.
- Meibohm, J., L. Pistone, K. Gustavsson, and B. Mehlig, 2017: Relative velocities in bidisperse turbulent suspensions. *Physical Review E*, **96** (6), 061 102.
- Onishi, R., and A. Seifert, 2016: Reynolds-number dependence of turbulence enhancement on collision growth. *Atmosph. Chemistry and Physics*, **16** (19), 12 441–12 455.
- Paoli, R., and K. Shariff, 2009: Turbulent condensation of droplets: direct simulation and a stochastic model. *Journal of the Atmospheric Sciences*, **66** (3), 723–740.
- Pinsky, M., and A. Khain, 2004: Collisions of small drops in a turbulent flow. part ii: Effects of flow accelerations. *J. Atmosph. Sci.*, **61** (15), 1926–1939.
- Pinsky, M., A. Khain, and H. Krugliak, 2008: Collisions of cloud droplets in a turbulent flow. part v: Application of detailed tables of turbulent collision rate enhancement to simulation of droplet spectra evolution. *J. Atmosph. Sci.*, **65** (2), 357–374.
- Pinsky, M., A. Khain, and M. Shapiro, 2007: Collisions of cloud droplets in a turbulent flow. part iv: Droplet hydrodynamic interaction. *J. Atmosph. Sci.*, **64** (7), 2462–2482.
- Pruppacher, H. R., and J. D. Klett, 2012: *Microphysics of Clouds and Precipitation: Reprinted 1980*. Springer Science & Business Media.
- Reuter, G., R. De Villiers, and Y. Yavin, 1988: The collection kernel for two falling cloud drops subjected to random perturbations in a turbulent air flow: a stochastic model. *J. Atmosph. Sci.*, **45** (5), 765–773.
- Rosa, B., H. Parishani, O. Ayala, W. W. Grabowski, and L.-P. Wang, 2013: Kinematic and dynamic collision statistics of cloud droplets from high-resolution simulations. *New J. Phys.*, **15** (4), 045 032.
- Saffman, P. G., and J. S. Turner, 1956: On the collision of drops in turbulent clouds. *J. Fluid Mech.*, **1**, 16–30, doi:10.1017/S0022112056000020, URL [http://journals.cambridge.org/article\\_S0022112056000020](http://journals.cambridge.org/article_S0022112056000020).
- Saito, I., and T. Gotoh, 2017: Turbulence and cloud droplets in cumulus clouds. *New Journal of Physics*.
- Salazar, J. P., J. De Jong, L. Cao, S. H. Woodward, H. Meng, and L. R. Collins, 2008: Experimental and numerical investigation of inertial particle clustering in isotropic turbulence. *J. Fluid Mech.*, **600**, 245–256.
- Sardina, G., F. Picano, L. Brandt, and R. Caballero, 2015: Continuous Growth of Droplet Size Variance due to Condensation in Turbulent Clouds. *Phys. Rev. Lett.*, **115** (18), 184501, doi:10.1103/PhysRevLett.115.184501, 1501.07051.
- Schiller, L., and A. Naumann, 1933: Fundamental calculations in gravitational processing. *Zeitschrift Des Vereines Deutscher Ingenieure*, **77**, 318–320.
- Shaw, R. A., 2003: Particle-turbulence interactions in atmospheric clouds. *Annu. Rev. Fluid Mech.*, **35** (1), 183–227.
- Shaw, R. A., W. C. Reade, L. R. Collins, and J. Verlinde, 1998: Preferential concentration of cloud droplets by turbulence: Effects on the early evolution of cumulus cloud droplet spectra. *J. Atmosph. Sci.*, **55** (11), 1965–1976.
- Shima, S., K. Kusano, A. Kawano, T. Sugiyama, and S. Kawahara, 2009: The super-droplet method for the numerical simulation of clouds and precipitation: a particle-based and probabilistic microphysics model coupled with a non-hydrostatic model. *Quart. J. Roy. Met. Soc.*, **135**, 1307–1320, physics/0701103.
- Siebert, H., K. Lehmann, and M. Wendisch, 2006: Observations of small-scale turbulence and energy dissipation rates in the cloudy boundary layer. *Journal of the atmospheric sciences*, **63** (5), 1451–1466.
- Siewert, C., J. Bec, and G. Krstulovic, 2017: Statistical steady state in turbulent droplet condensation. *Journal of Fluid Mechanics*, **810**, 254–280.
- Srivastava, R., 1989: Growth of cloud drops by condensation: A criticism of currently accepted theory and a new approach. *Journal of the atmospheric sciences*, **46** (7), 869–887.
- Stephens, G. L., and J. M. Haynes, 2007: Near global observations of the warm rain coalescence process. *Geophysical Research Letters*, **34** (20).
- Telford, J. W., 1955: A new aspect of coalescence theory. *Journal of Meteorology*, **12** (5), 436–444.
- Vaillancourt, P., M. Yau, P. Bartello, and W. W. Grabowski, 2002: Microscopic approach to cloud droplet growth by condensation. part ii: Turbulence, clustering, and condensational growth. *Journal of the atmospheric sciences*, **59** (24), 3421–3435.

- Vaillancourt, P., M. Yau, and W. W. Grabowski, 2001: Microscopic approach to cloud droplet growth by condensation. part i: Model description and results without turbulence. *Journal of the atmospheric sciences*, **58** (14), 1945–1964.
- Wang, L.-P., O. Ayala, S. E. Kasprzak, and W. W. Grabowski, 2005: Theoretical formulation of collision rate and collision efficiency of hydrodynamically interacting cloud droplets in turbulent atmosphere. *J. Atmosph. Sci.*, **62** (7), 2433–2450.
- Wang, L.-P., and W. W. Grabowski, 2009: The role of air turbulence in warm rain initiation. *Atmosph. Sci. Lett.*, **10** (1), 1–8.
- Wilkinson, M., 2016: Large deviation analysis of rapid onset of rain showers. *Phys. Rev. Lett.*, **116** (1), 018 501.
- Woittiez, E. J., H. J. Jonker, and L. M. Portela, 2009: On the combined effects of turbulence and gravity on droplet collisions in clouds: a numerical study. *Journal of the atmospheric sciences*, **66** (7), 1926–1943.
- Xue, Y., L.-P. Wang, and W. W. Grabowski, 2008: Growth of cloud droplets by turbulent collision–coalescence. *J. Atmosph. Sci.*, **65** (2), 331–356.
- Yau, M. K., and R. Rogers, 1996: *A short course in cloud physics*. Elsevier.
- Zsom, A., and C. P. Dullemond, 2008: A representative particle approach to coagulation and fragmentation of dust aggregates and fluid droplets. *Astron. Astrophys.*, **489** (2), 931–941.